Compression of interference patterns with application to phase-shifting digital holography

Emmanouil Darakis and John J. Soraghan

A compression method of phase-shifting digital holographic data is presented. Three interference patterns are recorded, and holographic information is extracted from them by phase-shifting interferometry. The scheme uses standard baseline Joint Photographic Experts Group (JPEG) or standard JPEG-2000 image compression techniques on the recorded interference patterns to reduce the amount of data to be stored. High compression rates are achieved for good reconstructed object image quality. The utility of the proposed method is experimentally verified with real holographic data. Results for compression rates using JPEG-2000 and JPEG of approximately 27 and 20, respectively, for a normalized root-mean-square error of ~0.7 are demonstrated. © 2006 Optical Society of America

OCIS codes: 040.1520, 050.5080, 090.1760, 090.2880, 100.2000, 110.3000.

1. Introduction

Holography[1] is a technique by which sufficient information on wavefronts emanating from objects is recorded to make possible the reproduction of three-dimensional views of these objects by reconstructing the corresponding wavefronts. The use of photosensitive recording materials such as photographic films to record such holograms introduces severe inflexibility for further processing because of long developing times and high cost, thus minimizing practical applications. Using digital holography,[2–5] in which the recording of the (digital) holograms is achieved by use of CCD devices and the reconstruction is performed by computers, reduces the recording time substantially while further digital processing is made possible, thus facilitating numerous practical applications.[5]

However, the digital holography method proposed above suffers from reduced reconstructed image quality, mainly owing to the presence of a zero-order term and the conjugate image that contaminates the reconstructed object's image. Several techniques[6–8] to eliminate these interference terms and hence to increase the resultant quality have been proposed. Using an off-axis recording setup can make the suppression of such terms easier; however, it increases the spatial resolution requirements, thus limiting its practical use given the relatively low resolution of the CCD sensors.

An alternative approach known as phase-shifting interferometry[9–11] has been introduced. With this method and by use of the phase-shifting interferometry algorithm the wavefront emanating from the object is directly calculated at the plane of the camera. Then, by appropriate propagation of this wavefront to a desired distance, the reconstructed object's image is obtained. With this technique an in-line recording setup can be used, reducing the spatial frequency of the hologram and hence reducing the requirement for high-resolution CCD sensors, whereas both the zero-order term and the conjugate image are suppressed, resulting in substantially increased quality. One disadvantage of the phase-shifting algorithm is the extra amount of calculation required during the recording. However, the major disadvantage is that with this method the complex wavefront has to be recorded, thus doubling the amount of data to be stored or transmitted, depending on the application. In addition, the recently introduced color phase-shifting digital holography,[12] in which one such wavefront is recorded for each of the three main colors (red, green, and blue), further increases the data storage and transmission bandwidth demands. As a result, effective holographic data compression becomes a critical issue.

The authors are with the Institute for Communications and Signal Processing, Department of Electronic and Electrical Engineering, University of Strathclyde, 204 George Street, Glasgow G1 1XW, UK. E. Darakis's e-mail address is emmdarakis@eee.strath.ac.uk.

Received 20 July 2005; revised 4 October 2005; accepted 5 November 2005; posted 14 November 2005 (Doc. ID 63592).

0003-6935/06/112437-07$15.00/0

The highly spatially uncorrelated speckle look of the wavefront and its complex nature substantially reduce the performance of compression techniques[13] such as the transform-based Joint Photographic Experts Group (JPEG) standard[14,15] that are commonly used for other image compression applications. Some non-transform-based techniques for the compression of a wavefront have been discussed in the literature.[16–19] The methods proposed make use of quantization, aiming to reduce the data volume. Although quantization is appropriate when robustness to error or low computation loads are of the most importance, this approach suffers from reduced effectiveness as well as reduced flexibility. This is so because the resultant quality falls rapidly as the bit depth decreases and because only specific, discrete, and usually crude steps of reduction of one or more bits per sample can be made. Compression of interference patterns has been studied in conventional (i.e., not phase-shifting) holography.[20] Mills and Yamaguchi[21] introduced compression of interference patterns in phase-shifting digital holography. However, quantization is used for compression in this case as well, reducing both the effectiveness of compression of this method and the resultant quality.

In this paper a scheme is presented wherein data compression is performed in the early stage of the procedure, when the data (interference patterns) still possess an imagelike appearance. This renders the use of standard compression techniques not only possible but, as is shown here, highly effective compared with previously proposed methods.

The paper is organized as follows: In Section 2 the phase-shifting interferometry hologram recording procedure is introduced, followed by a discussion of the compression approaches that have been used to date. In Section 3 we describe the new digital holographic compression method, explain the methodology, and discuss the results obtained in comparison with those of other existing approaches. Conclusions are given in Section 4.

2. Phase-Shifting Digital Holography

A. Hologram Recording and Reconstruction

Figure 1 shows a simplified in-line phase-shifting interferometry recording setup.[10,21] A laser beam of wavelength λ is split by a beam splitter into two paths. The first path contains the object to be recorded. Let the complex amplitude distribution of the light reflected from the object at its plane be

$$U_0(x', y') = A_0(x', y')\exp[i\phi_0(x', y')], \tag{1}$$

where $A_0(x', y')$ and $\phi_0(x', y')$ are the amplitude and the phase, respectively, of the wave at point (x', y'). The corresponding distribution at the plane of the CCD, which is a distance d_0 from the object, is given by the Fresnel–Kirchhoff diffraction integral,[22] also known as the Fresnel transform, that describes the propagation of the wave with the constant complex terms dropped for simplicity as

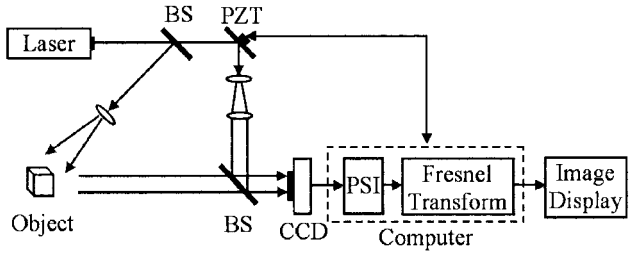

Fig. 1. Phase-shifting hologram recording and reconstruction setup: BS's beam splitters; PZT, piezoelectric transducer mirror; PSI, phase-shifting interferometry algorithm.

$$\begin{aligned} U(x, y) &= \int_{-\infty}^{+\infty}\int_{-\infty}^{+\infty} U_0(x', y')\exp\left\{\frac{ik}{2d_0}[(x-x')^2 \right. \\ &\quad \left. + (y-y')^2]\right\} dx'dy' \\ &= U_0 * G_{d_0}, \end{aligned} \tag{2}$$

where $k = 2\pi/\lambda$ is the wavenumber, $*$ denotes convolution, $G_d(x, y) = \exp[(ik/2d)(x^2 + y^2)]$ is a chirp function, and d is the propagation distance ($d = d_0$ in this case).

The other path contains a piezoelectric transducer mirror that phase modulates the laser beam. This device is appropriately controlled by a computer to apply a constant phase shift (steps $\phi = 0$, $\pi/2$, and π) to the beam. The phase-shifted reference wave can then be expressed as

$$U_R(x, y; \phi) = A_R(x, y)\exp(i\phi), \tag{3}$$

where $A_R(x, y)$ is the amplitude of the reference wave at point (x, y) and zero initial phase has been assumed for simplicity.

The phase-modulated beam is then superimposed upon the reflected wave from the object to form the interference pattern that is recorded at the plane of the CCD:

$$I(x, y; \phi) = |U_R(x, y; \phi) + U(x, y)|^2. \tag{4}$$

The computer combines the recorded interference patterns for each phase step, using the phase-shifting interferometry algorithm[21] to calculate the complex amplitude of the object wavefront as

$$\begin{aligned} U(x, y) = \frac{1-i}{4A_R}\{&[I(x, y; 0) - I(x, y; \pi/2)] \\ &+ i[I(x, y; \pi/2) - I(x, y; \pi)]\}. \end{aligned} \tag{5}$$

To reconstruct the object image we propagate this wavefront a distance d. We do this numerically by taking the Fresnel transform of the wavefront:

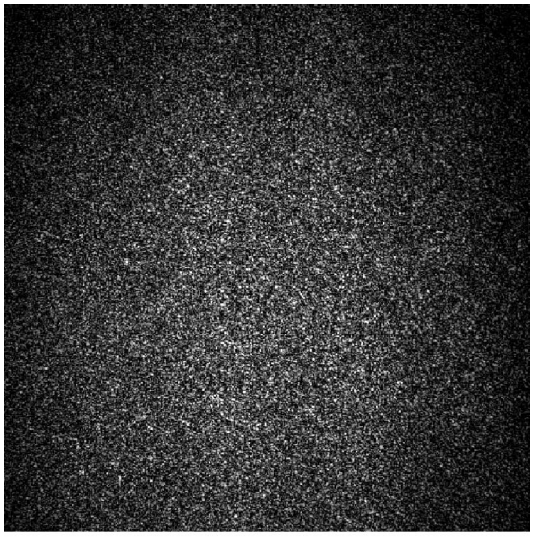

(a)

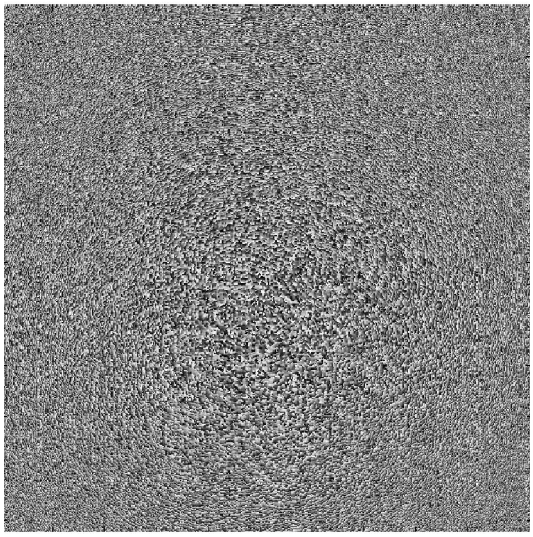

(b)

Fig. 2. (a) Magnitude and (b) phase of the measured wavefront (data courtesy of Fucai Zhang, Gunma University, Kiryu, Japan).

$$U'(X,\ Y,\ d) = \int_{-\infty}^{+\infty}\int_{-\infty}^{+\infty} U(x,\ y)\exp\left\{\frac{ik}{2d}\left[(X-x)^2 + (Y-y)^2\right]\right\}\mathrm{d}x\mathrm{d}y = U * G_d. \quad (6)$$

If Eq. (6) could be calculated over infinity and there were no quantization or other errors while the quantities were being measured, then the reconstructed object's image would be $U'(X, Y, -d_0) = U_0(x', y')$.

B. Wavefront Compression

A typical complex wavefront that results from the phase-shifting interferometry algorithm at the CCD plane is shown in Figs. 2(a) and 2(b) (amplitude and phase, respectively). Both the phase and the magnitude of this complex wavefront, which stores the actual three-dimensional information, are spatially highly uncorrelated; there is a lack of any noticeable structure. Thus the use of standard image compression algorithms for the compression of holographic data is highly ineffective.[13] The method shown in Fig. 3(a) and used by Naughton *et al.*[16–19] makes use of quantization on the complex wavefront to achieve reduction of the amount of data. Hence, for example, if the initial data were represented by 8 bits per sample, they would be truncated to 7, 6, 5, or even fewer bits per sample. In this way the amount of data is decreased, increasing the quantization error and hence substantially decreasing the quality of the reconstructed object, as Table 1 shows.

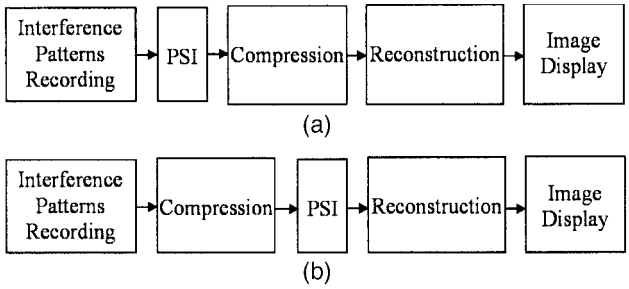

Fig. 3. Compression approaches: (a) complex wavefront compressed, (b) interference patterns compressed. PSIs, phase-shifting interferometry algorithms.

Although data compression is achieved in this way, this approach has several disadvantages. As indicated in Table 1, the compression rates achieved are very low, whereas the resultant quality decreases rapidly as the bit depth decreases. In addition, this approach suffers from inflexibility, given that only the specific quantization steps shown in Table 1 that correspond to integer multiples of 1 bit reduction can be taken. The use of arithmetic coding in addition to the quantization proposed[16,19] further increases the compression rates achieved. However, this increase is noteworthy only when a few bits per sample are retained, decreasing the dynamic range of the data. This increases the efficiency of the arithmetic coding but yields unacceptable reconstruction quality.

Table 1. Numerical Results of Quantization of the Complex Wavefront at the CCD Plane

Bits per Sample	Compression Rate	NRMS[a] Error
8	1	0
7	1.14	0.02
6	1.33	0.06
5	1.60	0.14
4	2	0.29
3	2.67	0.53
2	4	0.84
1	8	0.99

[a]NRMS, normalized root mean square.

3. Compressing the Interference Patterns

A. Methodology

Instead of following the procedure shown in Fig. 3(a), in which the highly uncorrelated complex wavefront is compressed, making quantization the only available compression choice, Mills and Yamaguchi[21] proposed the alternative procedure shown in Fig. 3(b). With the method proposed by them the interference patterns are subject to compression; however, quantization is still used to reduce the amount of data, leading to results similar to those described earlier, as can be seen from Table 2. The same disadvantages of low flexibility and reduced effectiveness remain with this method as well.

In Fig. 4(a) an interference pattern of an object (a die in this case) that corresponds to phase-shifting step $\phi = 0$ is shown. The interference patterns for the rest of the phase-shifting steps ($\phi = \pi/2$ and π) differ just slightly from that in Fig. 4(a) and hence are not shown here. The fact that the interference patterns are actual images captured by the CCD makes the use of more-sophisticated and hence more-effective (compared with quantization) compression methods possible.

In this paper we propose the use of baseline JPEG[14,15] and JPEG-2000[23,24] compression to reduce the data size of the interference patterns used for phase-shifting digital holography. Figure 4(b) shows the resultant interference pattern after the original has been compressed by use of the baseline JPEG algorithm. When this individual interference pattern is compressed at a rate of 29.17, a normalized root-mean-square (NRMS) error of 0.05 is observed. Although the introduced error is low, we have to investigate how this distortion of the interference patterns affects the quality of the image obtained at the plane of the object.

B. Experimental Setup and Numerical Calculations

To examine how the compression of interference patterns affects the quality of the reconstructed object we carried out the following measurements of real holographic data: An object (die) was positioned a distance $d_0 = 115$ mm approximately from a CCD camera and illuminated by a laser source radiating at $\lambda = 632.8$ nm. Three interference patterns, corresponding to phase-shift steps $\phi = 0, \pi/2,$ and π, were captured by the CCD camera. The camera had a resolution of 1024×1024 pixels pixels with a bit depth of 12 bits per pixel and a pixel pitch of 6.7 μm. The interference patterns recorded by the CCD are discrete, so Eq. (4) can be rewritten as

$$I(n, m; \phi) = |U_R(n, m; \phi) + U(n, m)|^2, \qquad (7)$$

where $n = 1, 2, \ldots, N_x$ and $m = 1, 2, \ldots, N_y$ are the discrete dimensions' indices. The bit depth of each of the interference patterns was then reduced to 8 bits per pixel, and appropriate scaling was carried out such that the full gray-scale range was covered, as shown in Fig. 4(a). These discrete interference patterns are taken as references. The discrete calculated

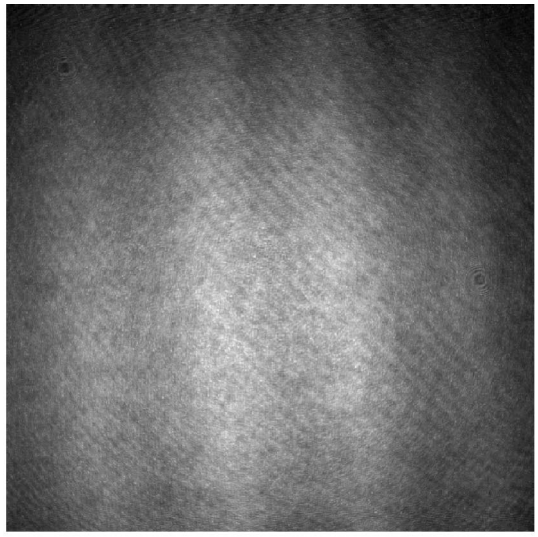

(a)

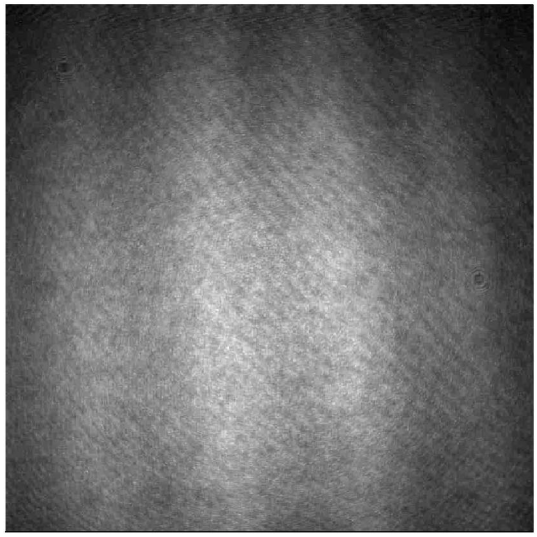

(b)

Fig. 4. One of the three interference patterns: (a) original interference pattern (data courtesy of Fucai Zhang, Gunma University, Kiryu, Japan), (b) the same interference pattern compressed by the JPEG algorithm.

Table 2. Numerical Results of Quantization of the Interference Patterns

Bits per Sample	Compression Rate	NRMS Error
8	1	0
7	1.14	0.03
6	1.33	0.06
5	1.60	0.13
4	2	0.3
3	2.67	0.86
2	4	2.33
1	8	5.74

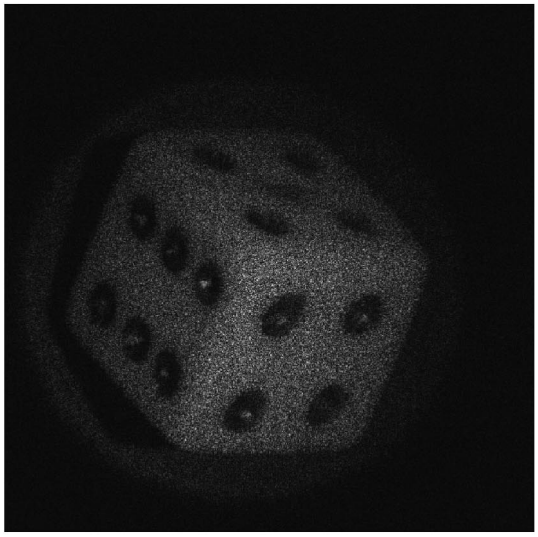

(a)

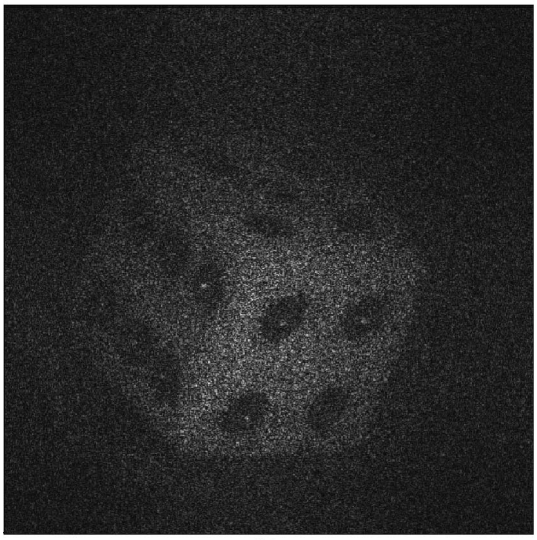

(b)

Fig. 5. Reconstructed object's images resulting (a) from the uncompressed interference patterns and (b) from the JPEG compressed interference patterns.

wavefront at the CCD plane is then given by

$$U(n,\ m) = \frac{1-i}{4A_R}\{[I(n,\ m;\ 0) - I(n,\ m;\ \pi/2)] + i[I(n,\ m;\ \pi/2) - I(n,\ m;\ \pi)]\}, \quad (8)$$

and the reference reconstructed object $U'(n, m, -d_0)$ shown in Fig. 5(a) is obtained by propagation of this wavefront to the appropriate distance, using a discrete version of Eq. (6).

The reference interference patterns $I(n, m; \phi)$ are compressed by use of the standard baseline JPEG as well as JPEG-2000 compression for several compression factors, giving $\hat{I}(n, m; \phi)$. The wavefront that results from these compressed interference patterns at the plane of the CCD, $\hat{U}(n, m)$, is then calculated from Eq. (8), where $\hat{I}(n, m; \phi)$ is to be used instead of $I(n, m; \phi)$. Finally, we obtain the reconstructed wavefront at the plane of the object, $\hat{U}'(n, m, -d_0)$, by taking the Fresnel transform of $\hat{U}(n, m)$, using Eq. (6) for an appropriate distance $d = -d_0$.

Table 3. Numerical Results of JPEG Compression

Total File Size (kBytes)	Compression Rate	NRMS Error
1864.63	1.1	0
1080.11	1.9	0.06
753.64	2.72	0.11
512.05	4	0.2
408.15	5.02	0.27
339.63	6.03	0.32
293.20	6.99	0.37
247.65	8.27	0.42
197.52	10.37	0.5
136.84	14.97	0.62
103.48	19.79	0.69
68.68	29.82	0.79
42.75	47.9	0.89
39.12	52.36	0.91

The NRMS error is used as a quantitive quality measure and is defined as follows:

$$D = \left\{\sum_{n=0}^{N_x-1}\sum_{m=0}^{N_y-1}\left[|U'(n,\ m,\ -d_0)|^2 - |\hat{U}'(n,\ m,\ -d_0)|^2\right]^2\right\}^{1/2} \times \left\{\sum_{n=0}^{N_x-1}\sum_{m=0}^{N_y-1}\left[|U'(n,\ m,\ -d_0)|^2\right]^2\right\}^{-1/2}. \quad (9)$$

The compression rate is calculated as follows:

$$r = \frac{\text{uncompressed size}}{\text{sum of compressed files' size}}, \quad (10)$$

where the sum of compressed files' size is the total of the three compressed interference pattern files' size. For the uncompressed size, the total size of the three uncompressed images could be used. These images have 1024 × 1024 pixels with 8 bits per pixel each, resulting in a total amount of 3 Mbytes. However, it can be argued that from these three interference patterns used for the phase-shifting algorithm a single complex wavefront of 1024 × 1024 samples with 8 bits per sample for each of the real and imaginary parts (2 MBytes in total) is obtained. Thus, given that these 2 MBytes of data are enough with which to reconstruct the object, assuming 8 bits per real and imaginary part of the initial uncompressed complex wavefront, the size of 2 MBytes is taken as the reference data size with which to calculate compression rates. As is shown in Subsection 3.C, the data reduction achieved by JPEG and JPEG-2000 compression is enough to bring the overall size of the three compressed interference patterns below 2 MBytes, and

Table 4. Numerical Results of JPEG-2000 Compression

Total File Size (kBytes)	Compression Rate	NRMS Error
1609.27	1.27	0
768.09	2.67	0.08
511.99	4	0.16
383.96	5.33	0.23
307.54	6.66	0.3
153.46	13.35	0.52
102.19	20.04	0.63
76.87	26.64	0.68
61.30	33.41	0.74
50.95	40.19	0.78
43.67	46.89	0.8
37.99	53.91	0.81
34.28	59.74	0.82
30.82	66.45	0.84
27.98	73.19	0.87
25.77	79.46	0.88
22.20	92.24	0.89
19.26	106.33	0.9
17.09	119.84	0.91
15.52	131.99	0.91
12.52	163.56	0.92

hence compression rates higher than 1 are achieved. Figure 5(b) shows an object image that results from the JPEG interference patterns compressed at a rate of 19.79, resulting in a NRMS error of 0.69.

C. Results and Discussion

In Tables 3 and 4 the numerical results obtained for JPEG and JPEG-2000 compression, respectively, are shown. The first row in each of the tables corresponds to lossless compression, and hence no NRMS error is introduced. It has to be mentioned that, because the JPEG-2000 standard can generally offer a greater range of compression rates, more measurements were taken in this case. In Fig. 6 the resultant compression rates are shown versus the obtained NRMS error for both JPEG and JPEG-2000 compression methods.

These results indicate that, for example, compression rates of approximately 20 and 27 can be obtained with the JPEG and JPEG-2000 methods, respectively, while a quality level of NRMS = 0.7 is retained. Compared with the compression rates and the resultant NRMS errors offered by the quantization approaches used by Naughton *et al.*[16–19] listed in Table 1 and that used by Mills and Yamaguchi[21] given in Table 2, this is a significant increase of compression ratio for a given quality.

It can be noted that, although in general the JPEG-2000 algorithm offers better compression quality for the same compression rate, this difference becomes apparent only for high compression rates at which the NRMS error is fairly high, and hence the reconstructed object quality may be considered unacceptable. As a result it can be claimed that, for imaging applications when the reconstructed object's quality

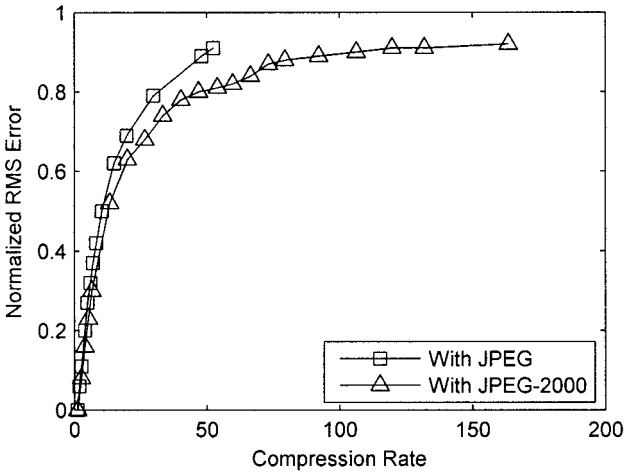

Fig. 6. NRMS error of the reconstructed image for several compression rates obtained with JPEG and JPEG-2000 compression.

is of highest interest, the use of the JPEG-2000 standard to compress the interference patterns offers only limited advantage over the baseline JPEG method.

The method proposed offers extensive flexibility in the choice of compression rates through a wide range of quality factor settings during the compression. Hence the trade-off limit between data reduction and the resultant quality can easily be set practically at any point required by a specific application.

In the preceding analysis the baseline JPEG and JPEG-2000 compression schemes were used and proved to be quite effective. However, a more careful selection of options, such as values of the quantization tables or wavelet filters used to match the special characteristics of the interference patterns, should further improve the resultant compression quality.

4. Conclusions

A digital holographic compression scheme based on standard image compression methods has been presented. Numerical evaluation has been performed by use of real holographic data for two compression algorithms, JPEG and JPEG-2000, and the quality of the reconstructed object's image has been measured for different compression rates. The numerical experiments indicate that approximate compression rates of 20 and 27 for the JPEG and JPEG-2000 algorithms, respectively, can be obtained while the reconstructed object's image quality remains at acceptable levels. By taking advantage of the ability to choose the quality factor offered by both JPEG and JPEG-2000 algorithms the new holographic compression method substantially increases flexibility by offering a wide range of compression rates for specific quality levels.

This study was supported by the Greek State Scholarships Foundation. The authors thank Fucai Zhang for kindly providing the holographic interference pattern data used for the experiments.

References

1. D. Gabor, "A new microscopic principle," Nature **161,** 777–778 (1948).
2. J. W. Goodman and R. Lawrence, "Digital image formation from electronically detected holograms," Appl. Phys. Lett. **11,** 77–79 (1967).
3. L. P. Yaroslavskii and N. S. Merzlyakov, *Methods of Digital Holography* (Consultants Bureau, 1980).
4. T. M. Kreis, M. Adams, and W. P. O. Juptner, "Methods of digital holography: a comparison," in *Optical Inspection and Micromeasurements II,* C. Gorecki, ed., Proc. SPIE **3098,** 224–233 (1997).
5. U. Schnars and W. P. O. Juptner, "Digital recording and numerical reconstruction of holograms," Meas. Sci. Technol. **13,** R85–R101 (2002).
6. T. M. Kreis and W. P. O. Juptner, "Suppression of the dc term in digital holography," Opt. Eng. **36,** 2357–2360 (1997).
7. E. Cuche, P. Marquet, and C. Depeursinge, "Spatial filtering for zero-order and twin-image elimination in digital off-axis holography," Appl. Opt. **39,** 4070–4075 (2000).
8. M. Liebling, T. Blu, and M. A. Unser, "Non-linear Fresnelet approximation for interference term suppression in digital holography," in *Wavelets: Applications in Signal and Image Processing X,* M. A. Unser, A. Aldroubi, and A. F. Laine, eds., Proc. SPIE **5207,** 553–559 (2003).
9. Y. Surrel, "Design of algorithms for phase measurements by the use of phase stepping," Appl. Opt. **35,** 51–60 (1996).
10. I. Yamaguchi and T. Zhang, "Phase-shifting digital holography," Opt. Lett. **22,** 1268–1270 (1997).
11. O. Matoba, T. J. Naughton, Y. Frauel, N. Bertaux, and B. Javidi, "Real-time three-dimensional object reconstruction by use of a phase-encoded digital hologram," Appl. Opt. **41,** 6187–6192 (2002).
12. I. Yamaguchi, T. Matsumura, and J. Kato, "Phase-shifting color digital holography," Opt. Lett. **27,** 1108–1110 (2002).
13. R. Shahnaz, J. F. Walkup, and T. F. Krile, "Image compression in signal-dependent noise," Appl. Opt. **38,** 5560–5567 (1999).
14. International Organization for Standardization (ISO)/International Electrotechnical Commission (IEC) standard 10918-1: 1994 for production of International Telecommunication Union Telecommunication Standardization Sector (ITU-T) recommendation T.81 (1994).
15. W. B. Pennebaker and J. L. Mitchell, *JPEG Still Image Data Compression Standard* (Van Nostrand Reinhold, 1993).
16. T. J. Naughton, Y. Frauel, O. Matoba, B. Javidi, and E. Tajahuerce, "Compression of digital holograms for three-dimensional video," in *Three-Dimensional Television, Video, and Display Technologies,* B. Javidi and F. Okano, eds. (Springer-Verlag, 2002), pp. 273–295.
17. T. J. Naughton, Y. Frauel, B. Javidi, and E. Tajahuerce, "Compression of digital holograms for three-dimensional object reconstruction and recognition," Appl. Opt. **41,** 4124–4132 (2002).
18. T. J. Naughton, J. B. McDonald, and B. Javidi, "Efficient compression of Fresnel fields for Internet transmission of three-dimensional images," Appl. Opt. **42,** 4758–4764 (2003).
19. T. J. Naughton and B. Javidi, "Compression of encrypted three-dimensional objects using digital holography," Opt. Eng. **43,** 2233–2238 (2004).
20. H. T. Chang, "Preliminary studies on compressing interference patterns in electronic holography," in *Three-Dimensional Holographic Imaging*, C. J. Kuo and M. H. Tsai, eds. (Wiley, 2002), pp. 99–117.
21. G. A. Mills and I. Yamaguchi, "Effects of quantization in phase-shifting digital holography," Appl. Opt. **44,** 1216–1225 (2005).
22. J. W. Goodman, *Introduction to Fourier Optics,* 3rd ed. (Roberts & Company, 2005).
23. International Organization for Standardization (ISO)/International Electrotechnical Commission (IEC) standard 15444-1: 2004 for production of International Telecommunication Union Telecommunication Standardization Sector (ITU-T) recommendation T.800 (2004).
24. T. Acharya and P.-S. Tsai, *JPEG2000 Standard for Image Compression: Concepts, Algorithms and VLSI Architectures* (Wiley, 2005).